J|A|C|S
COMMUNICATIONS

Published on Web 08/08/2006

Unique Contrast Patterns from Resonance-Enhanced Chiral SHG of Cell Membranes

Ping Yan, Andrew C. Millard, Meide Wei, and Leslie M. Loew*

Center for Cell Analysis and Modeling, University of Connecticut Health Center, Farmington, Connecticut 06030

Received May 22, 2006; E-mail: les@volt.uchc.edu

Second harmonic generation (SHG) is a nonlinear optical process in which two input photons generate one coherent output photon with twice the frequency. It is forbidden where there is an inversion symmetry, and this constraint makes it a sensitive tool for the study of interfaces and surfaces.[1,2] Special attention has been paid to the nonlinear effect of chiral molecules due to the fact that they are ubiquitous in biological systems and unable to form structures of inversion symmetry. Pioneering works on SHG from chiral surfaces and thin films,[3] sum frequency generation (SFG) from chiral solutions,[4] and SHG imaging of chiral surfaces[5] are beginning to establish a field of chiral-specific nonlinear spectroscopy and microscopy.[6]

Our laboratory has been exploring SHG as a new imaging contrast mechanism for cell structure and function.[7] The hemicyanine dye **1**, which we have called di-4-ANEPPDHQ,[8] is a typical dye designed as a probe for transmembrane electric potential because it displays a molecular Stark effect.[8−10] The underlying change in electron distribution between the ground and excited state is also a key prerequisite for resonance-enhanced SHG.[11] When the excitation wavelength is close to twice the absorption peak, resonance enhancements of the SHG by an order of magnitude are typical for arrays of such dyes bound to one leaflet of the lipid bilayer in the plasma membrane of a cell.[12] Utilizing the forward and backward light signals, respectively, SHG and two-photon fluorescence (2PF) images can be obtained simultaneously on a modified scanning confocal imaging system.[13−15] These two complementary imaging modalities have proven useful in understanding cell processes involving symmetry changes.[16] In earlier work, we appended chiral side chains to the hemicyanine chromophore and observed further enhancement of the resonance SHG signals.[15] In this communication, dimer **2** with the chiral center at the chromophore was synthesized. We find unique contrast patterns in images of cell membranes stained with chiral **2** compared to a racemic mixture or the achiral monomer **1**.

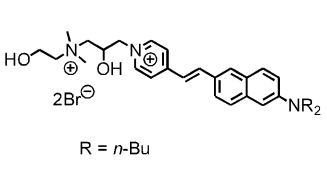

1

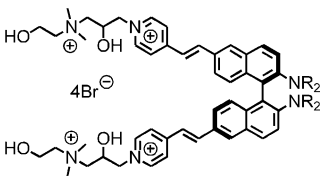

2

Binaphthyl derivatives have been the most popular model compounds for chiral SHG studies due to their strong chiral response and commercial availability.[3,5,17] As shown in Scheme 1, the synthesis of dimer **2** starts with (*R*)-1,1′-binaphthyl-2,2′-diamine, which is commercially available in optically pure form (Aldrich). Regiospecific bromination and reductive alkylation were achieved at low temperatures, and then the dibromide **5**, which is highly resistant to racemization at 110 °C, was coupled to vinyl pyridine and quaternized using the established methods for the monomer.[8] The CD spectrum of **2** (see Supporting Information) shows a large

Scheme 1 [a]

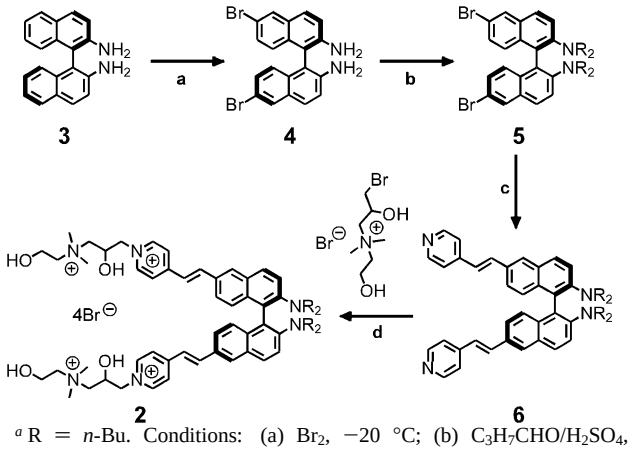

[a] R = *n*-Bu. Conditions: (a) Br_2, −20 °C; (b) C_3H_7CHO/H_2SO_4, $NaBH(OAc)_3$, rt; (c) $Pd(OAc)_2$, NEt_3, 110 °C; (d) DMF, 110 °C.

bisignate band, which is associated with exciton coupling of the long-axis polarized electronic transitions.[18] For comparison, racemic dimer was also synthesized starting from racemic 1,1′-binaphthyl-2,2′-diamine.

SHG intensity is governed by the second-order nonlinear susceptibility, χ_{ijk}, a third-rank tensor consisting of 27 elements.[19] A monolayer of achiral molecules belongs to $C_{\infty v}$ symmetry, and the tensor has three independent nonzero elements ($\chi_1 = \chi_{zzz}$, $\chi_2 = \chi_{zxx} = \chi_{zyy}$, $\chi_3 = \chi_{xzx} = \chi_{xxz} = \chi_{yzy} = \chi_{yyz}$); however, for chiral molecules, the monolayer belongs to C_∞ symmetry, and there is a fourth chiral element ($\chi_4 = \chi_{xyz} = \chi_{xzy} = -\chi_{yzx} = -\chi_{yxz}$).[19] The chiral SHG element can be separated and imaged by employing a special counter-propagating optical setup.[5]

However, a geometry that is commonly observed in cell cultures provides ready detection of chiral SHG. In a situation with two monolayers facing each other, as in the region of apposing membranes between adherent cells, all the achiral components cancel in the D_∞ symmetry.[20] Therefore, our nonlinear microscope can be used to directly image the remaining chiral SHG in such regions. Since the broad absorption bands for the monomer and the dimers have maxima at 473 and 449 nm, respectively, we used a Ti:sapphire laser tuned to 916 nm to effect resonance enhancement. Figure 1 shows SHG images (top panel) and 2PF images (bottom panel) of N1E-115 neuroblastoma cells stained with monomer, racemic dimer, and chiral dimer, respectively, from left to right. All three dyes can align well on the outer leaflets of cell membranes by virtue of their amphiphilic structures and produce strong SHG signals. The difference is rather subtle when looking at isolated single cells, but the effect of chirality manifests itself in the junction regions between two adherent cells: achiral SHG elements from two apposing cell membranes cancel, while chiral elements interfere constructively. As expected, there is little SHG signal from the junction parts of the cells stained with the monomer or racemic dimer (Figure 1a and 1b), while substantial signals can be observed for the chiral dimer (Figure 1c). 2PF is a noncoherent

10.1021/ja0635534 CCC: $33.50

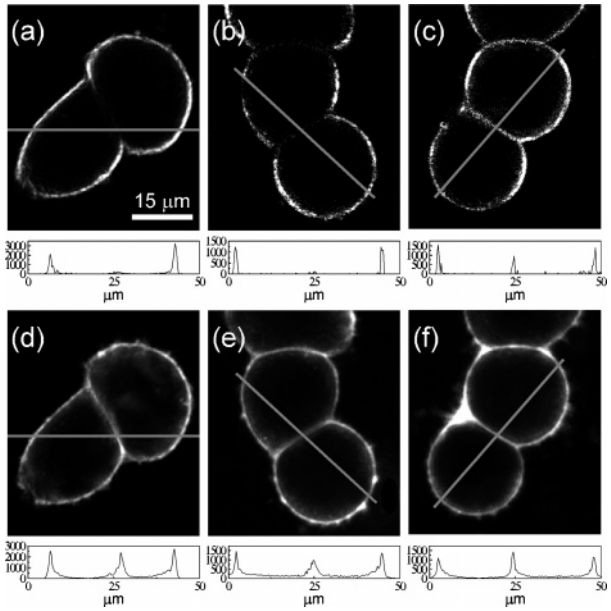

Figure 1. Effect of chirality on SHG imaging. (a−c) SHG and (d−f) 2PF images for cells stained with monomer (a, d), racemic dimer (b, e), or chiral dimer (c, f). Line scans through the junctions are shown at the bottom of each image. The samples were excited with circularly polarized light at a power level of ∼14 mW for the monomer and ∼28 mW for the dimers. Each image is a Kalman average of three acquisitions, corresponding to ∼8 s total acquisition time.

process, and the signals from the junction parts are strong for all cases (Figure 1d−f), indicating that these regions have ample dye densities that are comparable for all three dyes. For quantitative comparison, the SHG signals need to be normalized by the corresponding 2PF signals to account for the nonuniform staining. The ratio of junction/nonjunction SHG (normalized by 2PF) proves to be a reliable indicator of chirality: it is 0.10 ± 0.01 for the monomer ($N = 11$) and racemic dimer ($N = 16$), compared with 0.39 ± 0.04 for the chiral dimer ($N = 28$). Thus, resonance-enhanced chiral SHG expands the scope of SHG imaging to centrosymmetric structures.

The images in Figure 1 were obtained with circularly polarized incident light to avoid any asymmetries due to anisotropic cell geometry. We then explicitly investigated the contrast patterns that could be obtained with plane polarized light using the lymphocyte cell line L1210. These are small spherical (∼10 μm in diameter) cells with a convoluted membrane at the ultrastructural level, where the convolutions are at a distance scale shorter than the optical coherence length. Figure 2 shows SHG images from L1210 cells stained with either racemic or chiral **2** and imaged with either linearly polarized or circularly polarized light. The dependence of SHG on angle is manifest as arcs of intensity in the case of the racemic dye imaged with linearly polarized light. This corresponds to a preference for cell surface regions perpendicular to the electric field vector of the light, with the membrane convolutions effectively averaged out. There is no such clear spatial variation for the chiral dye and little difference between linear and circular polarization. This was the consistent pattern for all of several dozen cells examined. Thus, SHG is observed at all angles because the chiral component, χ_4, is not annihilated by the convoluted membrane. We see similar contrast patterns in the case of fluorescence, which also depends on angle but not on symmetry: sharp intensity arcs are often barely perceptible in cell membranes (see Supporting Information).

We have developed a new chiral chromophore that provides unique contrast patterns in resonance-enhanced SHG from stained

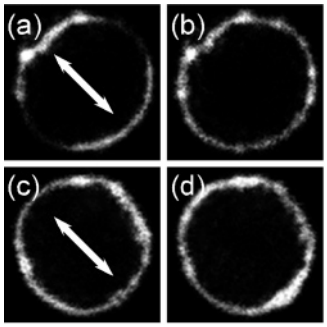

Figure 2. Effect of polarization on SHG imaging. Images (a) and (b) show one L1210 cell stained with racemic dimer; (c) and (d) show another cell stained with chiral dimer. Panels (a) and (c) were imaged using linearly polarized light, as shown by the arrow; (b) and (d) were imaged using circularly polarized light.

cell membranes. Chiral SHG allows imaging of D_∞ structures, which are not visible with traditional SHG. At the same time, chiral SHG possesses high selectivity: unlike fluorescence, it is still forbidden in isotropic solutions.[20] Biological structures, such as lipid bilayers, microfilaments, and microtubules, which are difficult or impossible to label noncentrosymmetrically, offer a rich basis for the application of chiral SHG. Indeed, chiral SHG fills a contrast niche among nonlinear optical probes: achiral SHG is specific for asymmetric interfaces; chiral SHG visualizes symmetric interfaces but is forbidden in isotropic solutions;[20] chiral SFG is allowed in chiral solutions;[4] 2PF is, of course, not subject to any symmetry constraints. Conversely, the variety of geometries offered by biological structures provides a rich basis for photophysical investigation of novel molecular arrays.

Acknowledgment. This study was supported by the National Institutes of Health via grant Nos. EB001963 and U54RR022232.

Supporting Information Available: Experimental section, including synthetic methods, CD spectra, microscope setup, and polarized 2PF images of cells in Figure 2. This material is available free of charge via the Internet at http://pubs.acs.org.

References

(1) Shen, Y. R. *Nature* **1989**, *337*, 519.
(2) Eisenthal, K. B. *Chem. Rev.* **1996**, *96*, 1343.
(3) (a) Hicks, J. M.; Petralli-Mallow, T. *Appl. Phys. B: Laser Opt.* **1999**, *68*, 589. (b) Verbiest, T.; Kauranen, M.; Persoons, A. *J. Mater. Chem.* **1999**, *9*, 2005.
(4) Ji, N.; Zhang, K.; Yang, H.; Shen, Y. R. *J. Am. Chem. Soc.* **2006**, *128*, 3482.
(5) Kriech, M. A.; Conboy, J. C. *J. Am. Chem. Soc.* **2005**, *127*, 2834.
(6) Simpson, G. J. *ChemPhysChem* **2004**, *5*, 1301.
(7) Campagnola, P. J.; Loew, L. M. *Nat. Biotechnol.* **2003**, *21*, 1356.
(8) Obaid, A. L.; Loew, L. M.; Wuskell, J. P.; Salzberg, B. M. *J. Neurosci. Methods* **2004**, *134*, 179.
(9) Loew, L. M.; Bonneville, G. W.; Surow, J. *Biochemistry* **1978**, *17*, 4065.
(10) Loew, L. M.; Scully, S.; Simpson, L.; Waggoner, A. S. *Nature* **1979**, *281*, 497.
(11) Dirk, C. W.; Twieg, R. J.; Wagniere, G. *J. Am. Chem. Soc.* **1986**, *108*, 5387.
(12) Williams, D. J. *Angew. Chem., Int. Ed. Engl.* **1984**, *23*, 690.
(13) Millard, A. C.; Campagnola, P. J.; Mohler, W.; Lewis, A.; Loew, L. M.; In *Methods in Enzymology*; Marriott, G., Parker, I., Eds.; Academic Press: San Diego, 2003; Vol. 361B, pp 47−69.
(14) Campagnola, P. J.; Clark, H. A.; Mohler, W. A.; Lewis, A.; Loew, L. M. *J. Biomed. Opt.* **2001**, *6*, 277.
(15) Campagnola, P. J.; Wei, M. D.; Lewis, A.; Loew, L. M. *Biophys. J.* **1999**, *77*, 3341.
(16) Millard, A. C.; Terasaki, M.; Loew, L. M. *Biophys. J.* **2005**, *88*, L46.
(17) Deussen, H. J.; Hendrickx, E.; Boutton, C.; Krog, D.; Clays, K.; Bechgaard, K.; Persoons, A.; Bjornholm, T. *J. Am. Chem. Soc.* **1996**, *118*, 6841.
(18) Berova, N.; Nakanishi, K. In *Circular Dichroism: Principles and Applications*; Berova, N., Nakanishi, K., Woody, R. W., Eds.; Wiley-VCH: New York, 2000; pp 337−382.
(19) Byers, J. D.; Yee, H. I.; Petrallimallow, T.; Hicks, J. M. *Phys. Rev. B* **1994**, *49*, 14643.
(20) Giordmaine, J. A. *Phys. Rev.* **1965**, *138*, A1599.

JA0635534